Large Transverse Energies and Jets in Hard Photoproduction at HERA [1]

Armen Buniatian

DESY, Notkestrasse 85, 22607 Hamburg, Germany
and Yerevan Physics Institute, Armenia

representing the H1 collaboration

ABSTRACT

Properties of the photoproduction events with large transverse energy in the hadronic final state are studied with H1 detector in three aspects: 1) distribution of transverse energy and energy flow, 2) multi-jet production and inclusive differential jet cross section, 3) properties of the energy flow in the central $\gamma p-$ collision and the $\gamma-$remnant region. Different QCD Monte Carlo models are compared with the measurements.

1. Introduction

The photoproduction of events with large observed transverse energy is one of the important research topics at the electron-proton collider HERA (26.7×820 GeV). The quasi-real photon is emitted by an electron, that is scattered through a small angle and is detected in an electron detector located $33m$ downstream the interaction region. For these events the virtuality of the photon is $3\times10^{-8} < Q^2 < 10^{-2}$ GeV^2/c^2. The photon energy is limited by the acceptance of the electron tagger to the range $0.25 \le y \le 0.7$, where $y \approx E_\gamma/E_e$, $E_\gamma = E_e - E_{e'}$, E_e and $E_{e'}$ are the energies of the incoming and outgoing electrons. The total energy of the photon-proton system is between 150 GeV and 250 GeV.

Two types of processes contribute to large E_T photoproduction: the incoming photon can interact either directly with a parton in the proton (*direct component*) or the photon acts as a source of partons which collide with the partons in the proton (*resolved component*). For leading order (LO) QCD the final state for pointlike scattering process consists of two partons with large transverse energies, that fragment into two jets of hadrons in addition to the proton remnant and the scattered electron which have small transverse energies. In the resolved process the spectator parton of the photon produces in addition a remnant jet with small transverse energy.

1.1 The Monte-Carlo Models

PYTHIA

Hard parton-parton interactions are generated with the PYTHIA[1] event generator using LO QCD matrix elements and including the initial and final state parton showers.

[1]Talk given at the International workshop PHOTON-95, Sheffield, UK, 8-13 April 1995

Since the QCD calculation is divergent for processes with small transverse momenta of the partons emerging from the hard interaction a lower cut-off of the $\hat{p}_t \geq 2$ GeV was set. For the proton and photon structure functions the leading order parameterizations GRV-LO were used[2]. Optionally, PYTHIA allows for interactions of partons from the photon remnant with partons from the proton remnant. This *multiple interaction* option has been explored in $p\bar{p}$ collisions before, the same parameters have been used here. The Lund fragmentation scheme as implemented in JETSET[3] was used for the hadronisation process.

PHOJET

The PHOJET MC event generator[4] is based on the two-component Dual Parton Model[5] incorporating soft hadronic processes, described by the supercritical Pomeron, and hard processes, described by perturbative constituent scattering. The hard processes are calculated with lower transverse momentum cut-off $\hat{p}_t \geq 3$ GeV. The soft interaction is represented by the multiple strings stretched between the proton and the resolved hadronic state of the photon. Multiple soft and hard interactions are the characteristic feature of this model. Their multiplicities are calculated within an unitarization scheme[6]. GRV-LO parameterizations[2] were used for the proton and photon structure functions. For the fragmentation process the JETSET[3] program was used.

1.2 The H1-Detector

The H1 detector is described in detail elsewhere[7]. Here we mention only the components of the detector relevant for this analysis.

The charged particle tracks and the interaction vertex are measured by a central and forward tracking system. The tracking region is surrounded by a fine grained liquid argon (LAr) calorimeter consisting of an electromagnetic section with lead absorber and a hadronic section with steel absorber. The calorimetric coverage is completed with a lead scintillator backward electromagnetic calorimeter in the electron direction. An electron tagger system allows tagging of electrons scattered at small angles ($< 5\ mrad$) from photoproduction processes, and is also used for luminosity measurement.

The following results are based on the data collected by H1 in 1993 and correspond to integrated luminosity $\int Ldt \approx 290\ nb^{-1}$.

2. Transverse Energy Flow and Cross-Section

The global measure of the rate of hard scattering processes is the differential transverse energy cross section

$$\frac{d^2\sigma}{d\eta^* dE_T}$$

Here $\eta^* = -\ln \tan\, \theta^*/2$ is the pseudorapidity in the γp CMS, the polar angle θ^* is measured with respect to the direction of outgoing proton, and E_T is the transverse energy in the pseudorapidity range $-2.5 < \eta^* < 1$. The measured E_T distribution was

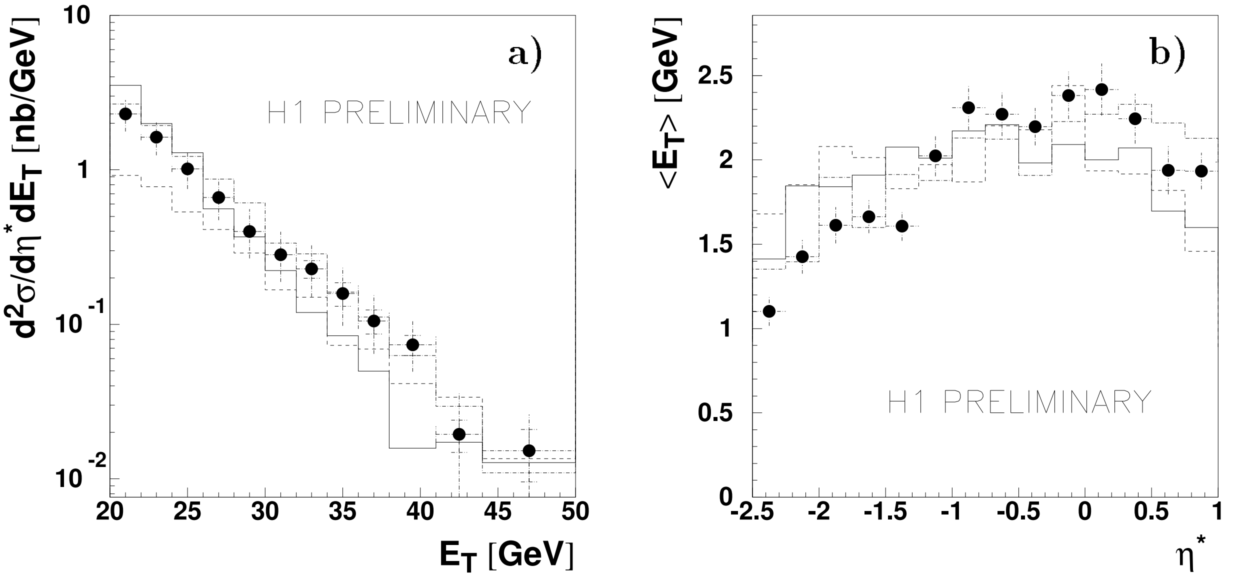

Figure 1: **a)** Transverse energy cross section integrated in the γp CMS pseudo-rapidity $-2.5 < \eta^* < 1$. **b)** The transverse energy flow in the range $-2.5 < \eta^* < 1$.
Points are H1 data. The solid line shows the predictions of the PYTHIA Monte Carlo with multiple interactions, the dashed line- PYTHIA without multiple interaction, and the dash-dotted line- PHOJET.

corrected for detector effects such, that we can compare it with the distributions of the transverse energy from the stable particles of Monte-Carlo events.

In Fig.1a the measured differential ep cross-section is compared with predictions of the PYTHIA and PHOJET Monte-Carlo generators. The inner error bars represent the statistical error, the outer error bars are the sum of statistical and systematic errors, added in quadrature. The dominant systematic error stems from a scale error for the hadronic energy in the LAr calorimeter. PYTHIA with multiple interactions and PHOJET describe the data well, but PYTHIA without multiple interactions predicts a smaller cross-section at small E_T.

Fig.1b shows the average transverse energy distribution for the photoproduction events with 25 GeV$< E_T <$ 30 GeV in the range $-2.5 < \eta^* < 1$ as function of η^*, corrected for detector effects. Only the statistical errors are shown. The distribution is approximately symmetric with respect to the γp CMS. PYTHIA fails to describe the data distribution, while PHOJET describes it well.

3. Jet Production

The production of jets reflects directly the parton-parton scattering processes. For the jet search we used a cone algorithm on a grid in pseudorapidity η and azimuthal angle φ with cone radius $R = \sqrt{\Delta\eta^2 + \Delta\varphi^2} = 1$. The transverse energies, pseudorapidities and azimuthal angles of the jets are calculated according to Snowmass convention[8].

The properties of the events containing jets were examined in terms of the transverse energy flow in the region around the jet axis. Fig.2 shows jet profiles for data and for PYTHIA in two ranges of η^{jet} for jets with transverse energy between 7 and 9 GeV as function of $\Delta\eta$ integrated over $|\Delta\varphi| < 1.0$. Here $\Delta\eta$ and $\Delta\varphi$ are the coordinates of the calorimeter cells relative to the jet axis. The MC describes the jet profile well in the direction of the photon ($\eta^{jet} < 0.5$). However, in the proton direction ($\eta^{jet} > 0.5$) the data show larger average values of E_T outside the jet cone than predicted by PYTHIA. Including multiple interactions improves the description but some difference between the data and Monte-Carlo still remains.

Fig.3 shows the relative numbers of jets with $E_T^{jet} \geq 7.0$ GeV and $-2.5 < \eta^{*\ jet} < 1$ per event as function of E_T, total transverse energy in the range $-2.5 < \eta^* < 1$. At $E_T \approx 20$ GeV more than 70% of the events have no jet. With increasing E_T the fraction of jet events increases. At $E_T \approx 40$ GeV almost all events have at least one jet, and more than 60% have two jets. In addition in Fig.3 the jet rates for the PYTHIA Monte-Carlo are shown. The development of jet rates with event E_T is quite similar to the data, however, it is evident that the fraction of MC events without jets is systematically lower.

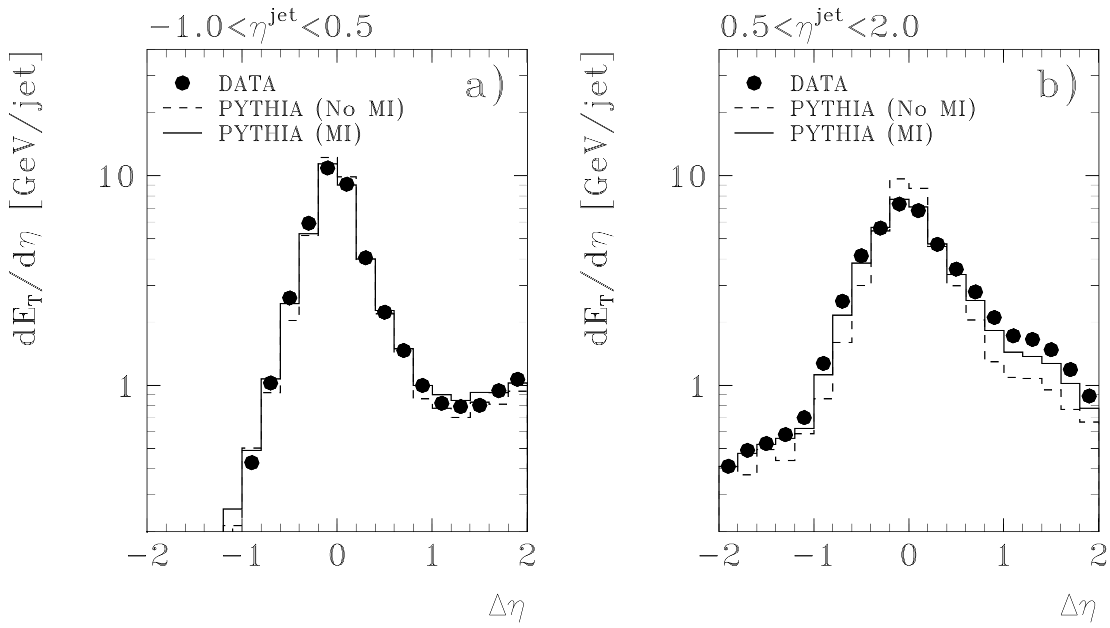

Figure 2: Transverse energy flow around the jet axis for jets with 7 GeV$\leq E_T^{jet} \leq 9$ GeV, and **a)** $-1 < \eta_{jet} < 0.5$ and **b)** $0.5 < \eta_{jet} < 2.0$

3.1 Inclusive Jet Cross-Section

The data sample with at least one jet with transverse energy $E_T^{jet} \geq 7$ GeV and jet axis in the pseudorapidity range $-1 \leq \eta^{jet} \leq 1.5$ was used for inclusive jet analysis. In total 2814 events containing 3166 jets satisfied the jet finding criteria. 2469 events in this sample contain 1 jet, 338 events contain 2 jets, and 7 events contain 3 jets. In order

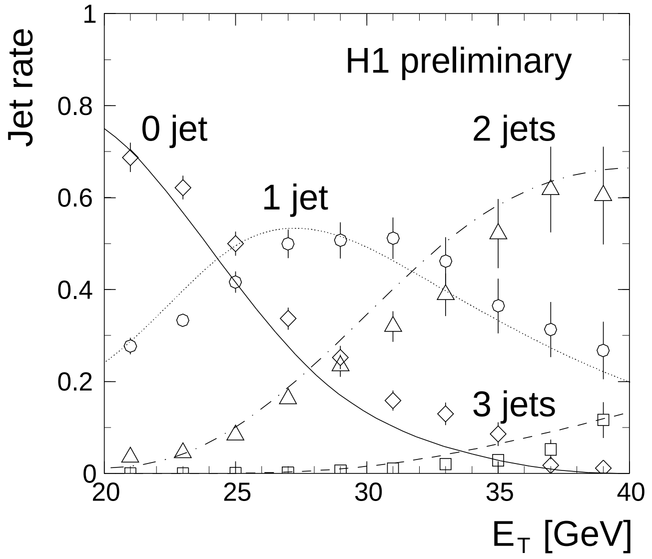

Figure 3: Relative rate of 0 (diamonds), 1 (circles), 2 (triangles), 3 (squares) jet events versus transverse energy in the range $-2.5 < \eta^* < 1$. Symbols are H1 data, curves are predictions of PYTHIA Monte-Carlo with multiple interactions.

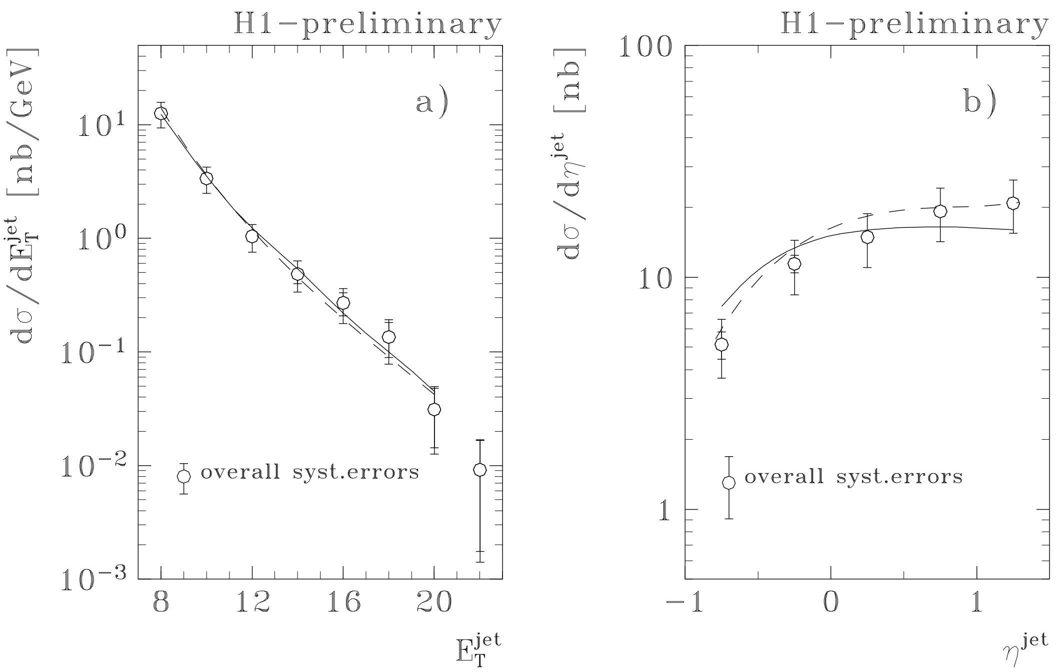

Figure 4: **a)** Inclusive jet E_T^{jet} cross-section integrated over the pseudorapidity interval $-1 \leq \eta^{jet} \leq 1.5$ and **b)** inclusive η^{jet} cross-section for jets with $E_T^{jet} \geq 7$ GeV. The curves are the predictions of the PYTHIA (solid) and PHOJET generators (dashed).

to obtain an inclusive jet cross-section, we corrected the observed jet rates for detector effects. Correction functions were derived by comparing the E_T^{jet} and η^{jet} distributions for jets in reconstructed Monte Carlo events with those of jets found from the original final state particles using the same jet algorithm as for reconstructed events. The corrected ep inclusive jet cross-section is shown in Fig.4, compared to PYTHIA and PHOJET Monte-Carlo predictions. The outer error bars show contributions from statistical errors and bin-by-bin systematic uncertainties, added in quadrature. The inner error bars represent only statistical errors. The overall systematic errors of the cross-section normalization amounts to $\pm 30\%$ and are shown separately. The cross-section $d\sigma/dE_T^{jet}$ shows a decrease with E_T^{jet} as $\sim E_T^{-5.5}$ and $d\sigma/d\eta^{jet}$ increases with η^{jet}. Both Monte-Carlo models describe the data within errors.

4. Energy Flow in the Central γp Collision Region and the Photon Remnant Region

The measurement of the dependence of transverse energy outside the jet cone on the momentum fraction of the parton from the photon, x_γ, is sensitive to a remnant-remnant interaction, since $1 - x_\gamma$ is proportional to the energy left in the photon remnant. For events with two jets in the final state, x_γ can be approximately reconstructed as $x_\gamma^{vis} \approx \sum(E_{T,i} \cdot e^{-\eta_i})/2E_\gamma$, where $E_{T,i}$ and η_i are the transverse energy and the pseudorapidity of two jets and E_γ is the photon energy[9]. Fig.5b shows the average transverse energy density $< E_T >$ in the photon remnant region ($\eta^* < -1$) as a function of x_γ^{vis} in the data and Monte-Carlo. The data exhibits a linear growth of $< E_T >$ with $1 - x_\gamma$, as expected qualitatively. All MC agree with data and with each other. This indicates that the multiple parton-parton interaction as modelled in PYTHIA and PHOJET do not add transverse energy into the $\gamma-$remnant region. In the central γp region ($-1 < \eta^* < 1$) the data again show a very clear rise with $1 - x_\gamma$ (Fig.5a). Now this rise is much steeper than for the Monte-Carlo without multiple interactions. Multiple interactions as modelled by PYTHIA add additional energy to the central γp region, but not enough at large $1 - x_\gamma$. PHOJET predicts an energy density outside the jets which is somewhat higher than in the data.

5. Summary

HERA photoproduction events with large observed transverse energy demonstrate the existence of hard scattering processes. We have studied various aspects of the transverse energy flow and jet production in our data and have compared then with Monte Carlo models. We find that:

- The differential transverse energy cross section agrees best with the PHOJET model.
- The energy flow measured versus rapidity is approximately symmetric with respect to the photon-proton CMS.
- The jet rate increases with the total transverse energy in the event. At large E_T 2-jet production dominates.
- The energy outside the jet peaks is asymmetric about the peak and is higher in the proton direction.
- In the $\gamma p-$central collision region the energy flow outside of the jets shows a steep linear dependence on the momentum fraction of the parton in the photon, suggestive of multiple parton-parton interactions.

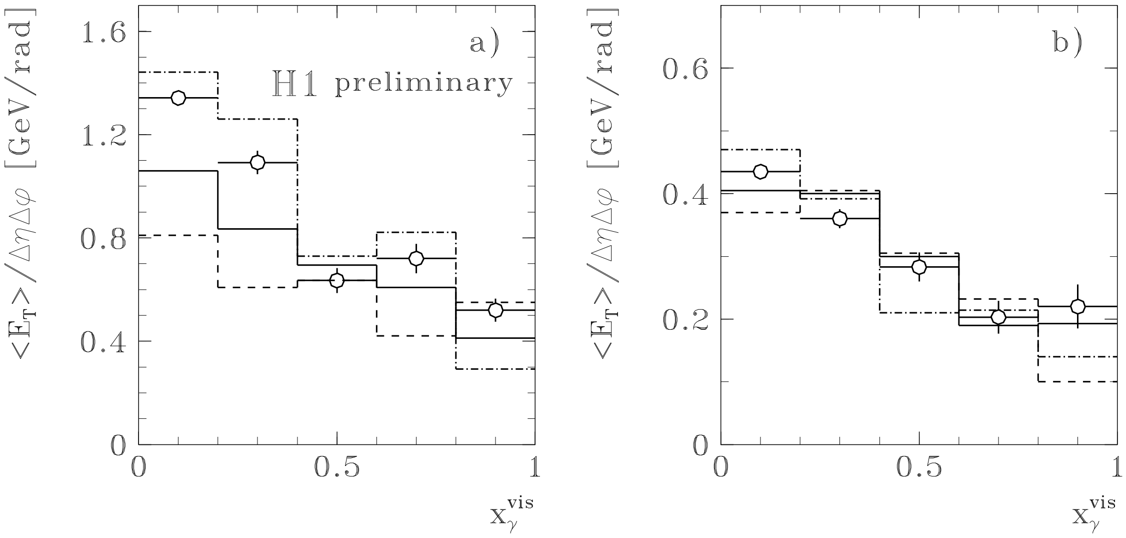

Figure 5: Observed transverse energy flow outside of the two jets versus the measured momentum fraction x_γ^{vis} in the **a)** central $\gamma p-$collision region ($-1 \leq \eta^* \leq 1$), and **b)** $\gamma-$remnant region ($\eta^* \leq -1$.) Circles are H1 data, the histograms are predictions of the PYTHIA generator with (solid line) and without multiple interactions (dashed line) and PHOJET generator (dash-dotted line).

- Only Monte-Carlo models which include multiple interactions give an acceptable description of the data.

6. References

1. T. Sjöstrand, *CERN-TH-6488* (1992)
2. M. Glück, E. Reya and A. Vogt, *Phys.Rev.* **D46** (1992) 1973
   M. Glück, E. Reya and A. Vogt, *Z. Phys.* **C53** (1992) 127
3. T. Sjöstrand, M.Bengtsson, *Comput.Phys.Commun.* **43** (1987)367
4. R. Engel, *In Proceedings of the XXIXth Rencontre de Moriond (1994)*, p.321.
5. A.Capella, et al, *Phys.Rep.* **236** (1994) 227.
6. P.Aurenche, et al, *Phys.Rev.* **D45** (1992) 92
   R.Engel, *Z.Phys.* **C66** (1995) 203
7. *The H1 detector at HERA*, DESY 93-103 (1993)
8. J. E. Huth et al., *Fermilab-Conf-90/249-E* (1990)
9. M. Erdmann (these proceedings)